ENVIRONMENTAL ENGINEERING SCIENCE
Volume 29, Number 7, 2012

DOI: 10.1089/ees.2010.0429

Process Conditions and Kinetics for the Removal of Copper from Water by Electrocoagulation

Subramanyan Vasudevan* and Jothinathan Lakshmi

Electro Inorganic Chemicals Division, CSIR—Central Electrochemical Research Institute, Karaikudi, India.

Received: November 23, 2010 *Accepted in revised form: April 19, 2011*

Abstract

The present study provides results from a study of the removal of copper from water through electrochemically generated Al^{3+} using aluminium alloy as the electrodes. Various operating conditions on the removal efficiency of copper were investigated, such as initial copper ion concentration, initial pH, current density, and temperature. Results showed that the optimum removal efficiency of 98.5% was achieved at a current density of 0.025 A/dm^2, at pH of 7.0. Effects of co-existing anions such as carbonate, phosphate, silicate, and fluoride were studied on the removal efficiency of copper. Results of pilot scale study show that the process was technologically feasible. Adsorption of copper could be described by the Langmuir adsorption isotherm suggesting monolayer coverage of adsorbed molecules. First- and second-order rate equations, Elovich and Intraparticle diffusion models, were applied to study adsorption kinetics. The adsorption process follows the second-order kinetics model with good correlation. Temperature studies showed that adsorption was endothermic and spontaneous in nature.

Key words: adsorption; aluminium alloy; copper removal; electrocoagulation; kinetics

Introduction

The presence of heavy metals in the aquatic environment is a source of great environmental alarm. Copper is known to be one of the heavy metals most toxic to living organisms, and it is one of the more widespread heavy metal contaminants of the environment (Vinikour *et al*., 1980; James *et al*., 2006). Copper, a metal that occurs naturally in rocks, soil, water, and air throughout the environment, is an essential element in plants, animals, and humans (Billon *et al*., 2006). The adverse health effects caused by copper, mercury, and arsenic poisoning are far more catastrophic than any other natural calamity throughout the world in recent times (Onmez and Aksu, 1999; Prasad and Freitas, 2000; Ozer *et al*., 2004). The potential sources of copper in industrial effluents include metal cleaning and plating baths, pulp, paper board mills, wood pulp production, fertilizer industry, paints and pigments, municipal and storm water run-off, and so on (Boujelben *et al*., 2009). The common symptoms of copper toxicity are injury to red blood cells and lungs, as well as damage to liver and pancreatic functions. Long-term exposure to copper can also cause irritation of the nose, mouth, and eyes, as well as headaches, stomachaches, dizziness, vomiting, and diarrhea (Gardea-Torresdey *et al*., 1996; Ajmal *et al*., 1998; Bailey *et al*., 1999; Yu *et al*., 2000; Ozcan *et al*., 2005). The drinking water guideline value recommended by the World Health Organization is 2 mg/L. The USEPA has set a maximum contaminant level of 1.3 mg/L for copper in drinking water (CPCB, 2002). Conventional methods for removing copper from water include ion exchange, reverse osmosis, co-precipitation, coagulation, electrodialysis, and adsorption (Shukla and Sakhardane, 1992; Villaescesa *et al*., 2004; Ozcan *et al*., 2005; Saeed *et al*., 2005; Fiol *et al*., 2006). Physical methods such as ion exchange, reverse osmosis, and electrodialysis have proved to be either too expensive or inefficient to remove copper from water. At present, chemical treatments are not used due to disadvantages such as high costs of maintenance, problems of sludge handling and its disposal, and neutralization of the effluent. The copper removal from water by adsorption using different materials has also been explored. The major disadvantages of this studied adsorbent are low efficiency and high cost. Recent research has demonstrated that electrocoagulation offers an attractive alternative to the above-mentioned traditional methods for treating water. In this process, anodic dissolution of metal electrode takes place with the evolution of hydrogen gas at the cathode. Electrochemically generated metallic ions from the anode can undergo hydrolysis to produce a series of activated intermediates that are able to destabilize the finely dispersed particles present in the water to be treated. The advantages of electrocoagulation include high-particulate removal efficiency, a compact treatment facility, relatively low cost, and the possibility of complete automation. This method is characterized by reduced sludge production, a minimum requirement of chemicals, and ease of operation (Mrozowski and Zielinski,

**Corresponding author:* Electro Inorganic Chemicals Division, CSIR—Central Electrochemical Research Institute, Karaikudi 630006, India. *Phone*: 91 (4565) 227556; *Fax*: 91 (4565) 227779; *E-mail:* vasudevan65@gmail.com

1983; Bailey *et al*., 1999; Adhoum and Monser, 2004; Chen, 2004; Carlos *et al*., 2006; Christensen *et al*., 2006; Miwa *et al*., 2006; Carlesi Jara *et al*., 2007; Onder *et al*., 2007). The reactions for aluminium electrode are as follows:

$$\text{At the anode} : \mathrm{Al} \rightarrow \mathrm{Al}^{3+} + 3\mathrm{e}^{-} \quad (1)$$

$$\text{At the cathode} : 2\mathrm{H_2O} + 2\mathrm{e}^{-} \rightarrow \mathrm{H_2(g)} + 2\mathrm{OH}^{-} \quad (2)$$

Although there are numerous reports related to electrochemical coagulation as a means of removal of many pollutants from water and wastewater, but there are limited works on copper removal by electrocoagulation method and its adsorption and kinetics studies. The present work provides an electrocoagulation process for the removal of copper from water using aluminium alloy as both anode and cathode. To optimize the maximum removal efficiency of copper, different parameters such as effect of initial concentration, effect of temperature, pH, and effect of current density were studied. In doing so, the equilibrium adsorption behavior is analyzed by fitting models of Langmuir, Freundlich, and Dubinin-Radushkevich (D-R) isotherms. Adsorption kinetics of electrocoagulants is analyzed using first-, second-order, Elovich, and Intraparticle models. Activation energy is evaluated to study the nature of adsorption.

Experimental Setup Methods

The electrochemical cell consisted of a 1.0 L glass vessel fitted with a PVC cover having suitable holes to introduce the electrodes, thermometer, pH sensor, and electrolyte. The anode and cathode with surface area of 0.2 dm^2 were made of aluminum alloy containing Zn (1%–4%), In (0.006%–0.025%), Fe (0.15%), and Si (0%–0.15%) supplied by CECRI, (CSIR), India, and placed at an inter-electrode distance of 0.005 m. The temperature of the electrolyte was controlled to the desired value with a variation of ± 2K by adjusting the rate of flow of thermostatically controlled water through an external glass-cooling spiral. A regulated direct current (DC) was supplied from a rectifier (10 A, 0–25 V; Aplab model).

Copper nitrate (Analar Reagent; Merck) was dissolved in deionized water for the required concentration of about 1.0 L. The pH of the electrolyte was adjusted, if required, with 1 M HCl or NaOH (Analar Reagent; Merck) solutions. Temperature studies were carried out at varying temperature (313K–343K) to determine the type of reaction. To examine the effect of co-existing ions, for the removal of copper, sodium carbonate, sodium phosphate, sodium silicate, and sodium fluoride were added to the electrolyte for required concentrations. All the experiments were repeated thrice for reproducibility, and the accuracy of the results are ± 1%.

The copper analysis was analyzed using UV-Visible Spectrophotometer (MERCK; Spectroquant Pharo 300). The scanning electron microscope (SEM) and EDAX of copper-adsorbed aluminium hydroxide coagulant were analyzed with an SEM made by Hitachi (model s-3000h). The XRD of electrocoagulatioan-by products were analyzed by a JEOL X-ray diffractometer (Type–JEOL). The Fourier transform infrared spectrum of aluminium hydroxide was obtained using Nexus 670 FTIR spectrometer (Thermo Electron Corporation). The concentration of carbonate, silicate, fluoride, and phosphate were determined using UV-Visible Spectrophotometer (MERCK; Pharo 300).

Result and Discussion

Effect of electrolyte pH

It has been established that the initial pH of the electrolyte is one of the important factors affecting the performance of the electrochemical process, particularly the performance of the electrocoagulation process. To evaluate its effect, a series of experiments were performed, using 10 mg/L copper-containing solutions, with an initial pH varying in the range of 4–12 at a current density of 0.025 A/dm^2. The removal efficiencies are 93, 96.8, 98.5, 98.3, 96.2, and 94.1 for pHs 4, 6, 7, 8, 10, and 12, respectively. The decrease of removal efficiency at more acidic and alkaline pH values has been observed by many investigators [Merzouk *et al.*, 2009; Zaied and Bellakhal 2009]; and it is attributed that at low pH, such as 2–3, cationic monomeric species Al^{3+} and $Al(OH)_2^+$ predominate. When pH is between 6 and 8, the Al^{3+} and OH^- ions generated by the electrodes react to form various monomeric species such as $Al(OH)_2^+$, $Al(OH)_2^{2+}$, and polymeric species such as $Al6(OH)_{15}^{3+}$, $Al_7(OH)_{17}^{4+}$, and $Al_{13}(OH)_{34}^{5+}$. These species finally transform into insoluble amorphous $Al(OH)_3$(s) through complex polymerization/precipitation kinetics. The formation of $Al(OH)_3$(s) is, therefore, optimal in the pH 7.

Effect of initial copper concentration

To study the effect of initial concentration, experiments were conducted at varying initial concentrations from 2 to 10 mg/L. The results are illustrated in Fig. 1. From the results, it can be seen that the adsorption of copper is increased with an increase in copper concentration and remains constant after equilibrium time. The equilibrium time was 5 min for all of the concentrations studied (2–10 mg/L). The amount of copper adsorbed (q_e) increased from 1.83 to 8.66 mg/g as the concentration was increased from 2 to 10 mg/L. The figure also shows that the adsorption is the rapid in the initial stages and gradually decreases with progress of adsorption. The plots are single, smooth, and continuous curves leading to saturation, suggesting the possible monolayer coverage to copper on the surface of the adsorbent.

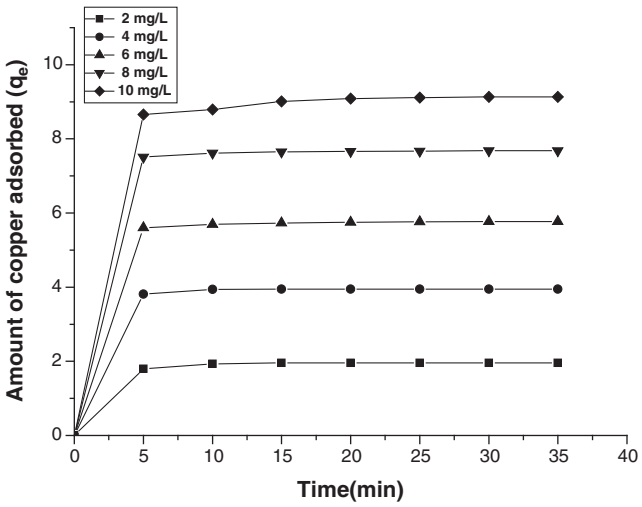

FIG. 1. Effect of agitation time and amount of copper adsorbed, at a current density of 0.025 A/dm^2, pH of 7.0, and temperature of 303 K.

Effect of current density

To investigate the effect of current density, a series of experiments were carried out using 10 mg/L of copper containing electrolyte, at a pH 7.0, with the current density being varied from 0.01 to 0.125 A/dm^2. The removal efficiencies of copper are 95.6%, 98.5%, 98.6%, 98.8%, 99.0%, and 99.1% for current densities 0.01, 0.025, 0.5, 0.075, 0.1, and 0.125 A/dm^2, respectively. It is found that, above 0.025 A/dm^2 the removal efficiency remains almost constant for higher current densities. So, further studies were carried out at 0.025 A/dm^2. The results showed that as current density increases, removal of copper also increases. This can be attributed to the increase in the amount of Al ions being generated *in situ*, thereby resulting in rapid removal of copper. The amount (average value) of adsorbent [$Al(OH)_3$] has been determined from the Faraday law:

$$E_c = ItM/ZF$$

where I is current in A, t is the time (s), M is the molecular weight, Z is the electron involved, and F is the Faraday constant (96,485.3 coulomb/mole). As expected, the amount of copper adsorption increases with the increase in adsorbent concentration, which indicates that the adsorption depends on the availability of binding sites for copper.

Effect of coexisting ions

Carbonate (HCO_3^-). The effect of (HCO_3^-) on copper removal was evaluated by increasing the (HCO_3^-) concentration from 0 to 250 mg/L in the electrolyte. The removal efficiencies are 98.5%, 96.2%, 83.0%, 69.1%, 36.0%, and 28.0% for the (HCO_3^-) ion concentration of 0, 2, 5, 65, 150, and 250 mg/L, respectively. From the results, it is found that the removal efficiency of the copper is not affected by the presence of (HCO_3^-) below 5 mg/L. Significant reduction in removal efficiency was observed above 5 mg/L of (HCO_3^-) concentration is due to the passivation of anode resulting, the hindering of the dissolution process of anode (Kabdasl *et al*., 2009).

Phosphate ($H_2PO_4^-$ and HPO_4^{2-}). The concentration of ($H_2PO_4^-$ and HPO_4^{2-}) ion was increased from 0 to 50 mg/L, the contaminant range of ($H_2PO_4^-$ and HPO_4^{2-}) in the ground water. The removal efficiency for copper was 98.5%, 95.3%, 78.3%, 59.1%, and 56.0% for 0, 2, 5, 25, and 50 mg/L of ($H_2PO_4^-$ and HPO_4^{2-}) ion, respectively. There is no change in removal efficiency of copper below 5 mg/L of ($H_2PO_4^-$ and HPO_4^{2-}) in the water. At higher concentrations (at and above 5 mg/L) of ($H_2PO_4^-$ and HPO_4^{2-}), the removal efficiency decreases to 50%. This is due to the preferential adsorption of ($H_2PO_4^-$ and HPO_4^{2-}) compared with copper as the concentration of ($H_2PO_4^-$ and HPO_4^{2-}) increases.

Silicate. The effect of silicate on the removal efficiency of copper was investigated. The respective efficiencies for 0, 5, 10, and 15 mg/L of silicate are 98.5%, 68.0%, 63.2%, and 59.0%. The removal of copper decreased with increasing silicate concentration from 0 to 15 mg/L. In addition to preferential adsorption, silicate can interact with aluminium hydroxide to form soluble and highly dispersed colloids that are not removed by normal filtration (Vasudevan *et al*., 2009).

Fluoride. From the results, it is found that the efficiency decreased from 98.5%, 90.0%, 76.3%, 59.0%, and 30.5% by increasing the concentration of fluoride from 0, 0.2, 0.5, 2, and 5 mg/L. This is due to the preferential adsorption of fluoride compared with copper as the concentration of fluoride increases. So, when fluoride ions are present in the water to be treated, they compete greatly with copper ions for the binding sites (Vasudevan *et al*., 2009).

Adsorption kinetics

First- and second-order rate equation. The variation of the adsorbed copper with time was kinetically characterized using the first- and second-order rate equation proposed by Lagergren. The first-order Lagergren model as (Ho and McKay, 1998; Wan Ngah and Hanafiah, 2008)

$$dq/dt = k_1(q_e - q_t) \tag{3}$$

where q_t is the amount of copper adsorbed on the adsorbent at time t (min), and k_1 (1/min) is the rate constant of first-order adsorption. The integrated form of the above equation with the boundary conditions $t = 0$ to > 0 ($q = 0$ to > 0) and then rearranged to obtain the following time-dependence function,

$$\log(q_e - q_t) = \log q_e - k_1 t/2.303 \tag{4}$$

where q_e is the amount of copper adsorbed at equilibrium. The q_e and rate constant k_1 were calculated from the slope of the plots of log ($q_e - q_t$) versus time (t) (figure not shown).

The second-order kinetic model is expressed as (Wu *et al*., 2005; Benaissa and Elouchdi, 2007)

$$dq/dt = k_2(q_e - q_t)^2 \tag{5}$$

Eq. (5) can be rearranged and linearized as

$$t/q_t = 1/k_2 q_e^{\,2} + t/q_e \tag{6}$$

where q_e and q_t are the amount of copper adsorbed on $Al(OH)_3$ (mg/g) at equilibrium and at time t (min),

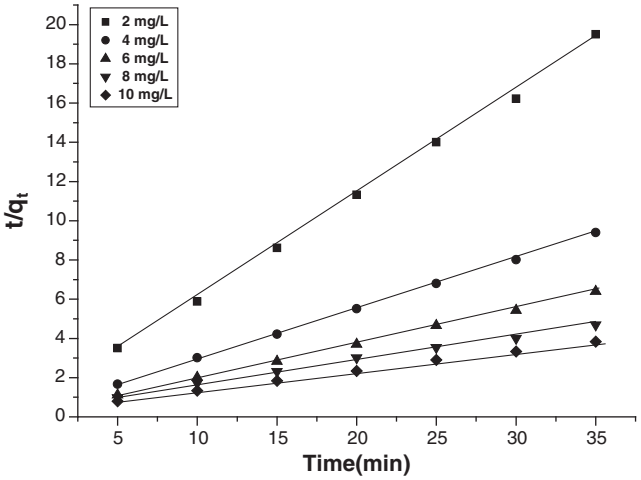

FIG. 2. Second-order kinetic model plot of different concentrations of copper at current density of 0.025 A/dm^2, temperature of 303K, and pH of 7.0.

Table 1. Comparison Between the Experimental and Calculated Q_E Values for Different Initial Copper Concentrations in First-Order and Second-Order Adsorption Kinetics at Room Temperature

Concentration (mg/L)	q_e *(exp) (mg/g)*	*First-order kinetics*			*Second-order kinetics*		
		q_e *(cal) (mg/g)*	k_1 *(min g/mg)*	R^2	q_e *(cal) (mg/g)*	k_2 *(min g/mg)*	R^2
2	1.83	1.0141	−0.0881	0.8564	1.8342	0.8426	0.9999
4	3.81	3.3442	−0.0331	0.8977	3.7766	0.3866	0.9976
6	5.62	4.9122	−0.1778	0.8124	5.5598	0.2647	0.9999
8	6.99	5.8447	−0.1987	0.8644	6.9124	0.0884	0.9983
10	8.66	7.6453	−0.2210	0.8467	8.6584	0.0761	0.9999

respectively, and k_2 is the rate constant for the second-order kinetic model. The equilibrium adsorption capacity, q_e (cal) and k_2, were determined from the slope and intercept of plot of t/q_t versus time (t) (Fig. 2) and are compiled in Table 1. The plots were found to be linear with good correlation coefficients (0.9999, 0.9976, 0.9999, 0.9983, and 0.9999 for 2, 4, 6, 8, and 10 mg/L initial copper concentration, respectively); and the theoretical q_e (cal) values agree well with the experimental q_e (exp) values at all concentrations studied. This implies that the second-order model is in good agreement with experimental data and can be used to favorably explain the copper adsorption in $Al(OH)_3$.

Elovich model and intraparticle diffusion

The simplified form of Elovich model is (Oke *et al*., 2008)

$$q_t = (1/\beta)\log_e(\alpha\cdot\beta) + (1/\beta)\log_e t \tag{7}$$

where α is the initial adsorption rate (mg/[g·h]), and β is the desorption constant (g/mg). If copper adsorption fits the Elovich model, a plot of q_t vs $\log_e$ (t) should yield a linear relationship with the slope of $(1/\beta)$ and an intercept of $(1/\beta)$ $\log_e$ $(\alpha\cdot\beta)$. Table 2 depicts the results obtained from Elovich equation. Lower regression value shows the inapplicability of this model.

Intraparticle diffusion is expressed as (Weber *et al*., 1963; Allen *et al*., 1989),

$$R = k_{id}(t)^{\alpha z} \tag{8}$$

A linearized form of Eq. (8) is followed by

$$\log R = \log k_{id} + a\log t \tag{9}$$

in which a depicts the adsorption mechanism, and k_{id} may be taken as the rate factor (percent of copper adsorbed per unit time). Lower and higher values of k_{id} illustrate an enhancement in the rate of adsorption and better adsorption with improved bonding.

Tables 1 and 2 depict the computed results obtained from first-order, second-order, Elovich and intraparticle diffusion. The correlation coefficient values decrease from second-order, first-order, and intraparticle diffusion to Elovich model. This indicates that the adsorption follows the second-order than the other models. Further, the calculated q_e values well agree with the experimental q_e values for second-order kinetics model than other models studied; and it is concluded that the second-order kinetics equation is the best-fitting kinetic model.

Adsorption isotherm

To determine the isotherms, the initial pH was kept at 7, and the concentration of copper used was in the range of 2–10 mg/L.

Freundlich isotherm

The mathematical expression of the Freundlich model can be written as (Lee *et al*., 2004; Prasanna Kumar *et al*., 2006)

$$q_e = KC^n \tag{10}$$

According to the Freundlich isotherm model, initially, the amount of adsorbed compounds increases rapidly; this increase slows down with the increasing surface coverage. Equation (10) can be linearized in logarithmic form, and the Freundlich constants can be determined as follows:

$$\log q_e = \log k_f + n\log C_e \tag{11}$$

where k_f is the Freundlich constant related to adsorption capacity n is the energy or intensity of adsorption; C_e is the

Table 2. Elovich Model and Intraparticle Diffusion for Different Initial Copper Concentrations at Temperature 305K and pH of 7

Concentration (mg/L)	*Elovich model*			*Intraparticle diffusion*		
	α *(mg/[g·h])*	β *(g/mg)*	R^2	k_{id} *(L/h)*	a *(%/h)*	R^2
2	8.11	61.27	0.7764	31.22	0.377	0.6568
4	4.35	40.27	0.7884	24.38	0.196	0.6455
6	2.99	26.33	0.7027	19.66	0.118	0.6879
8	0.98	15.14	0.7752	17.92	0.088	0.7788
10	0.84	9.22	0.6148	15.31	0.064	0.6012

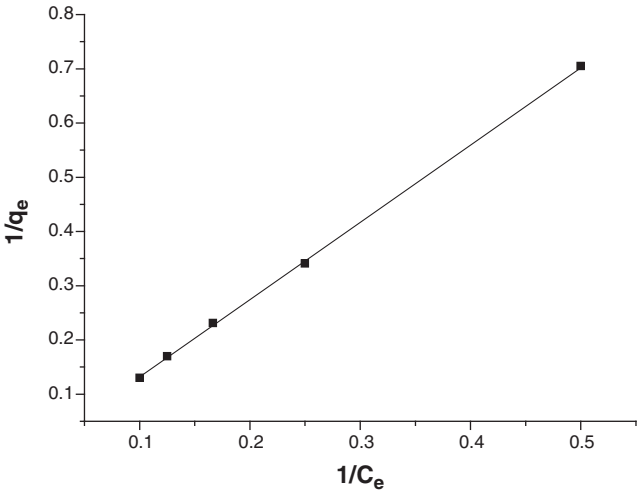

FIG. 3. Langmuir plot for adsorption of copper at pH of 7.0, current density of 0.025 A/dm^2, and temperature of 303K.

equilibrium concentration of copper (mg/L). In testing the isotherm, the copper concentration used was 2–10 mg/L; and at an initial pH 7, the adsorption data is plotted as log q_e versus log C_e and should result in a straight line with slope n and intercept k_f. The intercept and the slope are indicators of adsorption capacity and adsorption intensity, respectively. The value of n falling in the range of 1–10 indicates favorable sorption. The Freundlich constants k_f and n values are 0.9346 (mg/g) and 1.0011 (L/mg), respectively. From the analysis of the results, it is found that the Freundlich plots fit satisfactorily with the experimental data obtained in the present study.

Langmuir isotherm

The linearized form of Langmuir adsorption isotherm model is (Sarioglu *et al*., 2005; Bouzid *et al*., 2008)

$$C_e/q_e = 1/q_m b + C_e/q_m \tag{12}$$

where q_e is the amount adsorbed at equilibrium concentration C_e, q_m is the Langmuir constant representing maximum monolayer adsorption capacity, and b is the Langmuir constant related to energy of adsorption. The plots of $1/q_e$ as a function of $1/C_e$ for the adsorption of copper on $Al(OH)_3$ are shown in Fig. 3. The plots were found linear with good correlation coefficients (>0.99), indicating the applicability of the Langmuir model in the present study. The values of monolayer capacity (q_m) is found to be 203.91 mg/g, and Langmuir constant (b) is found to be 0.0018 L/mg. The values of q_m calculated by the Langmuir isotherm were all close to experimental values at given experimental conditions. These facts suggest that copper is adsorbed in the form of monolayer coverage on the surface of the adsorbent. The sorption isotherms of copper on aluminum hydroxide typically follow Langmuirian behavior as described by previous researchers (Sarioglu *et al*., 2005; Bouzid *et al*., 2008). The essential characteristics of the Langmuir isotherm can be expressed as the dimensionless constant R_L:

$$R_L = 1/(1 + bC_o) \tag{13}$$

where R_L is the equilibrium constant and indicates the type of adsorption, b is the Langmuir constant. C_o is various concentrations of copper solution. The R_L values between 0 and 1 indicate the favorable adsorption. The R_L values were found to be between 0 and 1 for all the concentrations of copper studied. The results are presented in Table 3.

D-R isotherm

This model is represented by (Tan *et al*., 2007),

$$q_e = q_s \exp(-B\varepsilon^2) \tag{14}$$

where $\varepsilon = RT \ln [1 + 1/C_e]$, B is related to the free energy of sorption per mole of the adsorbate as it migrates to the surface of the electrocoagulant from infinite distance in the solution, and q_s is the D-R isotherm constant related to the degree of

Table 3. Constant Parameters and Correlation Coefficient Calculated for Different Adsorption Isotherm Models at Different Temperatures for Copper Adsorption on Aluminium Hydroxide

Isotherm	*Constants*			
Langmuir	q_m (mg/g)	b (L/mg)	R_L	R^2
	203.91	0.0018	0.8847	0.9999
Freundlich	k_f (mg/g)	n (L/mg)		R^2
	0.9346	1.0011		0.9899
D-R	q_s ($\times 10^3$ mol/g)	B ($\times 10^3$ mol^2/kJ^2)	E (kJ/mol)	R^2
	1.5547	2.0154	9.04	0.9017

Table 4. Pore Diffusion Coefficients for the Adsorption of Copper at Various Concentrations and Temperature

	Pore diffusion constant $D \times 10^{-9}$ *(cm^2/s)*
Concentration (mg/L)	
2	1.001
4	0.994
6	0.832
8	0.804
10	0.766
Temperature (K)	
313	1.066
323	0.946
333	0.884
343	0.739

Table 5. Thermodynamic Parameters for the Adsorption of Copper

Temperature (K)	K_c	ΔG^o *(kJ/mol)*	ΔH^o *(kJ/mol)*	ΔS^o *(J/[mol·K])*
313	0.2881	−740.22	18.664	0.06876
323	0.5534	−1563.25		
333	0.8975	−2184.87		
343	1.3844	−2887.44		

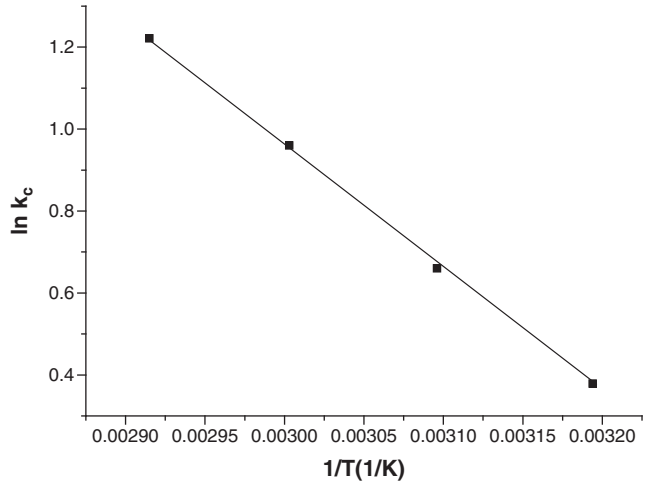

FIG. 4. Plot of log k_c and $1/T$ at pH of 7.0, current density of 0.025 A/dm^2.

adsorbate adsorption by the adsorbent surface. The linearized form of Equation (14) is

$$\ln q_e = \ln q_s - 2B \cdot RT \ln (1 + 1/C_e) \tag{15}$$

The isotherm constants of q_s and B are obtained from the intercept and slope of the plot of ln q_e versus ε^2 respectively (Demiral *et al*., 2008). The constant B gives the mean free energy E, of adsorption per molecule of the adsorbate when it is transferred to the surface of the solid from infinity in the solution and the relation is given as

$$E = 1/\sqrt{2B} \tag{16}$$

The magnitude of E is useful for estimating the type of adsorption process. It was found to be 9.04 kJ/mol. So, the type of adsorption of copper on aluminium hydroxide was defined as chemical adsorption.

The correlation coefficient values of different isotherm models are listed in Table 3. The Langmuir isotherm model has a higher regression coefficient ($R^2 = 0.999$) when compared with the other models, indicating that the Langmuir model provides a better description of the process.

Effect of temperature

The amount of copper adsorbed on the adsorbent increases by increasing the temperature, thus indicating the process to be endothermic. The diffusion co-efficient (D) for intraparticle transport of copper species into the adsorbent particles has been calculated at different temperature by

$$t_{1/2} = 0.03 \times {r_o}^2/D \tag{17}$$

where $t_{1/2}$ is the time of half adsorption (s), r_o is the radius of the adsorbent particle (cm), and D is the diffusion co-efficient in cm^2/s. For all chemisorption systems, the diffusivity co-efficient should be 10^{-5} to 10^{-13} cm^2/s (Yang and Al-Duri, 2001). In the present work, D is found to be in the range of 10^{-10} cm^2/s. The pore diffusion coefficient (D) values for various temperatures and different initial concentrations of copper are presented in Table 4.

To find out the energy of activation for adsorption of copper, the second-order rate constant is expressed in Arrhenius form (Golder *et al*., 2006),

$$\ln k_2 = \ln k_o - E/RT \tag{18}$$

where k_o is the constant of the equation (g/[mg·min]), E is the energy of activation (J/mol), R is the gas constant (8.314 J/[mol·K]), and T is the temperature in K. The activation energy (0.396 kJ/mol) is calculated from the slope of the fitted equation from the plot log k_2 versus $1/T$. The free energy change is obtained using the following relationship,

$$\Delta G = -RT \ln K_c \tag{19}$$

where ΔG is the free energy (kJ/mol), K_c is the equilibrium constant, R is the gas constant, and T is the temperature in K. The K_c and ΔG values are presented in Table 5. From the table, it is found that the negative value of ΔG indicates the spontaneous nature of adsorption. Other thermodynamic parameters such as entropy change (ΔS) and enthalpy change (ΔH) were determined using the van't Hoff equation,

$$\ln K_c = \frac{\Delta S}{R} - \frac{\Delta H}{RT}. \tag{20}$$

The enthalpy change ($\Delta H = 18.664$ kJ/mol) and entropy change ($\Delta S = 0.06878$ kJ/mol) were obtained from the slope and intercept of the van't Hoff linear plots of ln K_c versus $1/T$ (Fig. 4). Positive value of enthalpy change (ΔH) indicates that the adsorption process is endothermic in nature, and the negative value of change in internal energy (ΔG) shows the spontaneous adsorption of copper on the adsorbent. Positive values of entropy change show the increased randomness of the solution interface during the adsorption of copper on the adsorbent (Table 5). Enhancement of adsorption capacity of electrocoagulant (aluminium hydroxide) at higher

TABLE 6. COMPARISON BETWEEN EXPERIMENTAL AND CALCULATED Q_E VALUES FOR DIFFERENT INITIAL COPPER CONCENTRATIONS OF 10 MG/L IN FIRST- AND SECOND-ORDER ADSORPTION KINETICS AT VARIOUS TEMPERATURES AND pH OF 7

		First-order adsorption			*Second-order adsorption*		
Temperature (K)	q_e *(exp)*	q_e *(cal)*	K_1 *(min/mg)*	R^2	q_e *(cal)*	K_2 *(min/mg)*	R^2
313	7.99	1.667	−0.0037	0.7864	7.978	0.0997	0.9999
323	8.88	2.117	−0.0028	0.6055	8.798	0.1873	0.9988
333	9.24	3.279	−0.0015	0.7642	9.225	0.2446	0.9973
343	9.36	4.225	−0.0013	0.7886	9.336	0.3054	0.9999

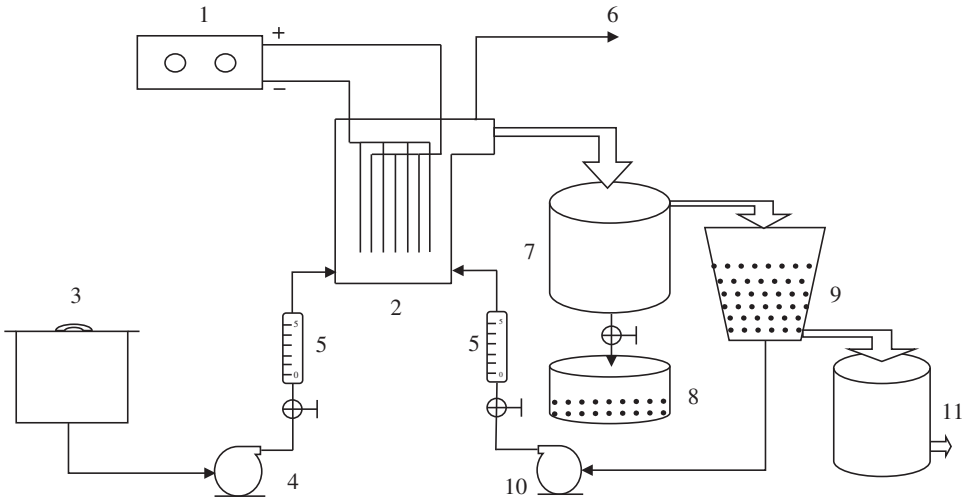

FIG. 5. Flow diagram of pilot plant electrochemical system. 1, direct-current power supply; 2, electrocoagulation cell; 3, water tank; 4, inlet pump; 5, flow meter; 6, gas outlet; 7, settling tank; 8, sludge collection tank; 9, filtration unit; 10, recirculation pump; 11, treated water.

temperatures may be attributed to the enlargement of pore size and or activation of the adsorbent surface. Using Lagergren rate equation, first-order rate constants and correlation co-efficient were calculated for different temperatures (305K–343K). The calculated q_e values obtained from the second-order kinetics agree with the experimental q_e values better than the first-order kinetics model. Table 6 depicts the computed results obtained from the second-order kinetic models. These results indicate that the adsorption follows the second-order kinetic model at different temperatures used in this study.

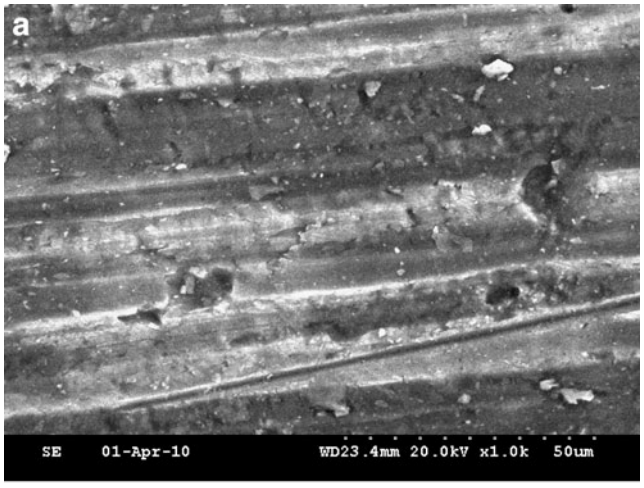

FIG. 6. Scanning electron microscope image of the anode **(a)** before and **(b)** after treatment.

A pilot plant study

A pilot plant capacity cell (Fig. 5) was designed, fabricated, and operated for the removal of copper from water. The system consists of a direct-current power supply, an electrochemical reactor, a water tank, a feed pump, a flow control valve, a flow measuring unit, a circulation pump, settling tank, sludge collection tank, filtration unit provisions for gas outlet, and treated water outlet. The reactor is made of PVC with an active volume of 1000 L. The electrode sets (anode and cathode) each consist of five pieces of aluminum alloy sheets, situated approximately 5 mm apart from each other and submerged in the solution. The total electrode surface area is 1340 cm^2 for both cathodes and anodes. The cell was operated at a current density of 0.025 A/dm^2 and an electrolyte pH of 7.0. The results showed that the maximum removal efficiency of 97.0% was achieved at a current density of 0.025 A/dm^2 and a pH of 7 using aluminium alloy as the anode and the

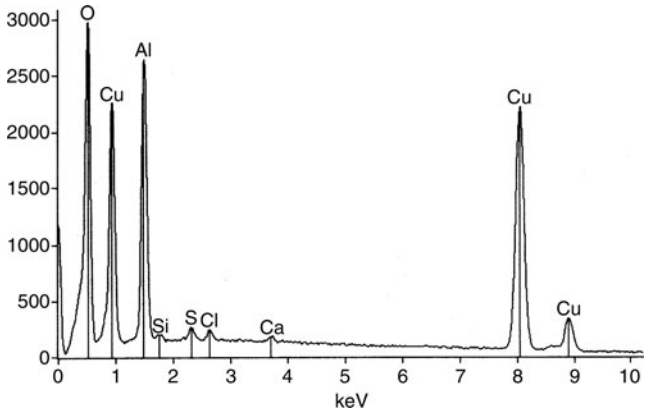

FIG. 7. Energy dispersive x-ray analysis (EDAX) for copper-adsorbed electrocoagulant.

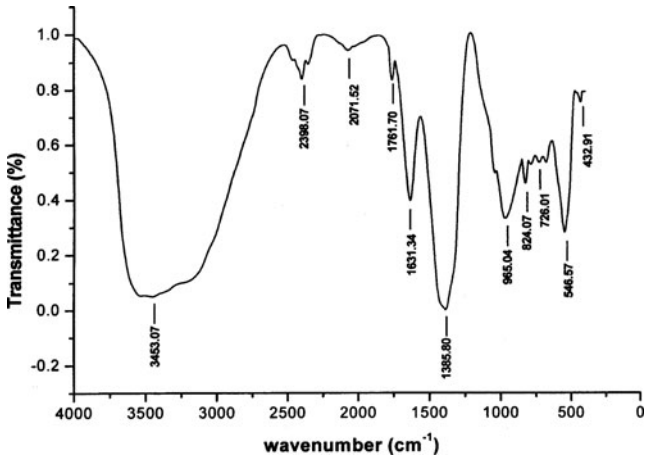

FIG. 8. Fourier transform infrared spectroscopy (FTIR) spectrum for copper-adsorbed electrocoagulant.

cathode. The results were consistent with the results obtained from the laboratory scale, showing that the process was technologically feasible.

Surface morphology

SEM and EDAX studies. SEM images of aluminum anode, before and after electrocoagulation of copper electrolyte, were obtained to compare the surface texture. Figure 6a shows the original aluminum plate surface before its use in electrocoagulation experiments. The surface of the electrode is uniform. Figure 6b shows the SEM of the same electrode after several cycles of use in electrocoagulation experiments. The electrode surface is now found to be rough, with a number of dents. These dents are formed around the nucleus of the active sites where the electrode dissolution results in the production of aluminum hydroxides. The formation of a large number of dents may be attributed to the anode material consumption at active sites due to the generation of oxygen at its surface.

Energy-dispersive analysis of X-rays was used to analyze the elemental constituents of copper-adsorbed aluminium hydroxide shown in Fig. 7. It shows that the presence of Cu, Al, and O appears in the spectrum. EDAX analysis provides direct evidence that copper is adsorbed on aluminium hydroxide. Other elements detected in the adsorbed aluminum hydroxide come from adsorption of the conducting electrolyte, chemicals used in the experiments, alloying, and the scrap impurities of the anode and cathode.

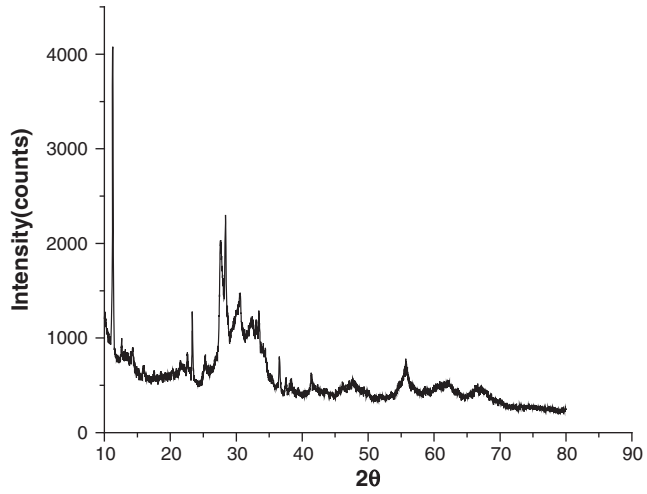

FIG. 9. X-ray difraction (XRD) spectrum for copper-adsorbed electrocoagulant.

Fourier transform infrared spectroscopy (FTIR) analysis. Figure 8 presents the FTIR spectrum of copper–aluminum hydroxide. The sharp and strong peak at 3453.07 cm^{-1} is due to the O–H stretching vibration in the $Al(OH)_3$ structures. The 1631.34 cm^{-1} peak indicates the bent vibration of H–O–H. The strong peak at 955.04 cm^{-1} is assigned to the Al–O–H bending. Cu–O vibration at 824 cm^{-1} is also observed.

XRD analysis. X-ray diffraction spectrum (Fig. 9) of aluminum electrode coagulant showed very broad and sallow diffraction peaks. This broad hump and low intensity indicate that the coagulant is amorphous or very poor crystalline in nature. It is reported (Gross *et al.*, 2007) that the crystallization of aluminum hydroxide is a very slow process resulting in all aluminum hydroxides found to be either amorphous or very poorly crystalline. The literature on the amorphous nature of aluminum oxide layer supported the present results.

Conclusions

The results showed that the optimized removal efficiency of 98.5% was achieved at a current density of 0.025 A/dm^2 and pH of 7.0 using aluminium alloy as both anode and cathode. The aluminium hydroxide generated in the cell removes the copper present in the water and reduces the copper concentration to less than 1 mg/L, thus making it fit for drinking. The results showed that the process was technologically feasible at a cost of 1.02 $kW \cdot h/m^3$. Langmuir adsorption isotherm was found to fit the equilibrium data for copper adsorption. The adsorption process follows second-order kinetics. Temperature studies showed that adsorption was endothermic and spontaneous in nature.

Acknowledgment

The authors wish to express their gratitude to the Director, Central Electrochemical Research Institute, Karaikudi, for aid in publishing this article.

Author Disclosure Statement

No competing financial interests exist.

Nomenclature

a: the adsorption mechanism
A: initial adsorption rate
b: free energy of sorption per mole of the adsorbate
B: desorption constant
C_e: equilibrium concentration of copper
C_o: initial concentration of copper
D: diffusion co-efficient
E: mean free energy
F: Faraday constant
I: current
k_1: First order rate constant

k_2: second order rate constant
k_a: energy of adsorption
k_f: Freundlich constant related to adsorption capacity
k_{id}: percent of copper adsorbed per unit time
k_o: constant of the equation
M: molecular weight
n: energy or intensity of adsorption
q_e: amount of copper adsorbed
q_m: adsorption capacity (Langmuir constant)
q_s: Dubinin-Radushkevich (D-R) isotherm constant
q_t: amount of copper adsorbed on the adsorbent at time t
R: gas constant
R_L: equilibrium constant
r_o: radius of the adsorbent particle
t: time
$t_{1/2}$: time of half adsorption
T: temperature
Z: number of electrons involved
ΔG: free energy
ΔH: enthalpy change
ΔS: entropy change

References

Adhoum, N., and Monser, L. (2004). Decolourization and removal of phenolic compounds from olive mill wastewater by electrocoagulation. *Chem. Eng. Process* 43, 1281.

Ajmal, M., Khan, A., Ahmad, S., and Ahmad, A. (1998). Role of sawdust in the removal of copper (II) from industrial wastes. *Water Res.* 32, 3085.

Allen, S.J., McKay, G., and Khader, K.H.Y. (1989). Intraparticle diffusion of basic dye during adsorption onto sphagnum peat. *Environ. Pollut.* 56, 39.

Bailey, S.E., Olin, T.J., Bricka, R.M., and Adrian, D.D. (1999). A review of potentially low-cost sorbents for heavy metals. *Water Res.* 33, 2469.

Benaissa, H., and Elouchdi, M.A. (2007). Removal of copper ions from aqueous solutions by dried sunflower leaves. *Chem. Eng. Process* 46, 614.

Billon, L., Meric, V., Castetbon, A., Francois, J., and Desbrieres, J. (2006). Removal of copper ions from water of boilers by a modified natural based Corncobs L. *J. Appl. Poly. Sci.* 102, 4637.

Boujelben, N., Bouzid, J., and Elouear, Z. (2009). Adsorption of nickel and copper onto natural iron oxide-coated sand from aqueous solutions: study in single and binary systems. *J. Hazard. Mater.* 163, 376.

Bouzid, J., Elouear, Z., Ksibi, M., Feki, M., and Montiel, A. (2008). A study on removal characteristics of copper from aqueous solution by sewage sludge and pomace ashes. *J. Hazard. Mater.* 152, 838.

Carlesi Jara, D., Fino, V., Specchia, G., and Saracco, P. (2007). Electrochemical removal of antibiotics from wastewaters. *Appl. Catal. B Environ.* 70, 479.

Carlos, A., Huitle, M., and Ferro, S. (2006). Electrochemical oxidation of organic pollutants for the wastewater treatment: direct and indirect processes. *Chem. Soc. Rev.* 35, 1324.

Chen, G. (2004). Electrochemical technologies in wastewater treatment. *Sep. Purif. Technol.* 38, 11.

Christensen, P.A., Egerton, T.A., Lin, W.F., Meynet, P., Shaoa, Z.G., and Wright, N.G. (2006). A novel electrochemical device for the disinfection of fluids by OH radicals. *Chem. Commun.* 38, 4022.

CPCB. (2002). Central Pollution Control Board, Government of India, Delhi. www.cpcb.nic.in

Demiral, H., Demiral, I., Tumsek, F., and Karacbacakoglu, B. (2008). Adsorption of chromium (Vl) from aqueous solution by activated solution by activated carbon derived from olive bagasse and applicability of different adsorption models. *Chem. Eng. J.* 44, 188.

Fiol, N., Villaescesa, I., Martınez, M., Miralles, N., Poch, J., and Serarols, J. (2006). Sorption of Pb(II), Ni(II), Cu(II) and Cd(II) from aqueous solutions by olive stone waste. *Sep. Purif. Technol.* 50, 132.

Gardea-Torresdey, J.L., Tang, L., and Salvador, J.M. (1996). Copper adsorption by esterified and unesterified fractions of *Sphagnum* peat moss and its different humic substances. *J. Hazard. Mater*. 48, 191.

Golder, A.K., Samantha, A.N., and Ray, S. (2006). Removal of phosphate from aqueous solution using calcined metal hydroxides sludge waste generated from electrocoagulation. *Sep. Purif. Technol*. 52, 102.

Gross, U., Rüdiger, S., Kemnitz, E., Brzezinka, K.W., Mukhopadhyay, S., Bailey, W.A., and Harrison, N. (2007). Vibrational analysis study of aluminium trifluoride phases. *J. Phys. Chem. A* 111, 5813.

Ho, Y.S., and McKay, G. (1998). A comparison of chemisorption kinetic models applied to pollutant removal on various sorbents. *Process Saf. Environ. Prot.* 76, 332.

James, R., Sampath, K., and Selvamani, P. (2006). Effect of ion-exchanging agent, zeolite on removal of copper in water and improvement of growth in *Oreochromis mossambicus* (Peters). *Asian Fish. Sci*. 13, 317.

Kabdasl, I., Vardar, B., Arslan-Alaton, I., and Tunay, O. (2009). Effect of dye auxiliaries on color and COD removal from simulated reactive dyebath effluent by electrocoagulation. *Chem. Eng. J.* 148, 89.

Lee, C.I., Yang, W.F., and Hsieh, C.I. (2004). Removal of copper (II) by manganese-coated sand in a liquid fluidized-bed reactor. *J. Hazard. Mater.* B114, 45.

Merzouk, B., Gourich, B., Sekki, A., Madani, K., Vial, C., and Barkaoui, M. (2009). Studies on the decolorization of textile dye wastewater by continuous electrocoagulation process. *Chem. Eng. J.* 149, 207.

Miwa, D.W., Malpass, G.R.P., Machado, S.A.S., and Motheo, A.J. (2006). Electrochemical degradation of carbaryl on oxide electrodes. *Water Res.* 40, 3281.

Mrozowski, J., and Zielinski, J. (1983). Studies of zinc and lead removal from industrial wastes by electrocoagulation. *Environ. Prot. Eng*. 9, 77.

Oke, I.A., Olarinoye, N.O., and Adewusi, S.R.A. (2008). Adsorption kinetics for arsenic removal from aqueous solutions by untreated powdered eggshell. *Adsorption* 14, 73.

Onder, E., Koparal, A.S., and Ogutveren, U.B. (2007). An alternative method for the removal of surfactants from water: electrochemical coagulation. *Sep. Purif. Technol*. 52, 527.

Onmez, G., and Aksu, Z. (1999). The effect of copper (II) ions on the growth and bioaccumulation properties of some yeasts. *Process Biochem.* 35, 35.

Ozcan, A., Ozcan, A.S., Tunali, S., Akar, T., and Kiran, I. (2005). Determination of the equilibrium, kinetic and thermodynamic parameters of adsorption of copper (II) ions onto seeds of capsicum annuum. *J. Hazard. Mater.* B124, 200.

Ozer, A., Ozer, D., and Ozer, A. (2004). The adsorption of copper (II) ions onto dehydrated wheat bran (DWB): determination of the equilibrium and thermodynamic parameters. *Process Biochem*. 39, 2183.

Prasad, M.N.V., and Freitas, H. (2000). Removal of toxic metals from solution by leaf, stem and root phytomass of *Quercus ilex* L. (holly oak). *Environ. Pollut.* 110, 277.

Prasanna Kumar, Y., King, P., and Prasad, V.S.R.K. (2006). Removal of copper from aqueous solution using *Ulva fasciata* sp.—A marine green algae. *J. Hazard. Mater.* B137, 367.

Saeed, A., Iqbal, M., and Akhtar, M.W. (2005). Removal and recovery of lead (II) from single and multimetal (Cd, Cu, Ni, Zn) solutions by crop milling waste (black gram husk). *J. Hazard. Mater*. B117, 65.

Sarioglu, M., May, A., and Cebeci, Y. (2005). Removal of copper from aqueous solutions by phosphate rock. *Desalination* 181, 303.

Shukla, S.P., and Sakhardane, V.D. (1992). Column studies on metal ion removal by dyed cellulosic materials. *J. Appl. Poly. Sci*. 44, 903.

Tan, I.A.W., Hameed, B.H., and Ahmed, A.L. (2007). Equilibrium and kinetics studies on the basic dye adsorption by palm fiber activated carbon. *Chem. Eng. J*. 127, 111.

Vasudevan, S., Lakshmi, J., Jayaraj, J., and Sozhan, G. (2009). Remediation of phosphate-contaminated water by electrocoagulation with aluminium, aluminium alloy and mild steel anodes. *J. Hazard. Mater.* 164, 1480.

Vinikour, W.S., Goldstein, R.M., and Anderson, R.V. (1980). Bioaccumulation patterns of zinc, copper, cadmium and lead in selected fish species from the Fox River, Illinois. *Bull. Environ. Contam. Toxicol*. 24, 727.

Villaescesa, I., Fiol, N., Martinez, M., Miralles, N., Poch, J., and Serarols, J. (2004). Removal of copper and nickel ions from aqueous solutions by grape stalk wastes. *Water Res.* 38, 992.

Wan Ngah, W.S., and Hanafiah, M.A.K.M. (2008). Adsorption of copper on rubber (*Hevea brasiliensis*) leaf powder: Kinetic, equilibrium and thermodynamic studies. *Biochem. Eng. J.* 39, 521.

Weber, W.J., Jr., and Morris, J.C. (1963). Kinetics of adsorption on carbon from solutions. *J. Sanit. Div. ASCE* 89, 31.

Wu, Z., Joo, H., and Lee, K. (2005). Kinetics and thermodynamics of the organic dye adsorption on the mesoporous hybrid xerogel. *Chem. Eng. J*. 112, 227.

Yang, X.Y., and Al-Duri, B. (2001). Application of branched pore diffusion model in the adsorption of reactive dyes on activated carbon. *Chem. Eng. J*. 83, 15.

Yu, B., Zhang, Y., Shukla, A., Shukla, S.S., and Dorris, K.L. (2000). The removal of heavy metal from aqueous solutions by sawdust adsorption-removal of copper. *J. Hazard. Mater.* 80, 33.

Zaied, M., and Bellakhal, N. (2009). Electrocoagulation treatment of black liquor from paper industry. *J. Hazard. Mater.* 163, 995.